

Modelling framework for dynamic interaction between multiple pedestrians and vertical vibrations of footbridges

Original

Modelling framework for dynamic interaction between multiple pedestrians and vertical vibrations of footbridges / Venuti, Fiammetta; Racic, Vitomir; Corbetta, Alessandro. - In: JOURNAL OF SOUND AND VIBRATION. - ISSN 0022-460X. - ELETTRONICO. - 379:(2016), pp. 245-263. [10.1016/j.jsv.2016.05.047]

Availability:

This version is available at: 11583/2645268 since: 2016-07-19T10:14:08Z

Publisher:

Elsevier, Academic Press

Published

DOI:10.1016/j.jsv.2016.05.047

Terms of use:

This article is made available under terms and conditions as specified in the corresponding bibliographic description in the repository

Publisher copyright

Elsevier postprint/Author's Accepted Manuscript

© 2016. This manuscript version is made available under the CC-BY-NC-ND 4.0 license
<http://creativecommons.org/licenses/by-nc-nd/4.0/>. The final authenticated version is available online at:
<http://dx.doi.org/10.1016/j.jsv.2016.05.047>

(Article begins on next page)

Modelling framework for dynamic interaction between multiple pedestrians and vertical vibrations of footbridges

Fiammetta Venuti^{a,*}, Vitomir Racic^{b,c}, Alessandro Corbetta^{d,a}

^aPolitecnico di Torino, Department of Structural, Building and Geotechnical Engineering, Corso Duca degli Abruzzi 24, I-10129, Torino, Italy

^bPolitecnico di Milano, Department of Civil and Environmental Engineering, Piazza Leonardo da Vinci 32, I-20133, Milano, Italy

^cUniversity of Sheffield, Department of Civil and Structural Engineering, Sir Frederick Mappin Building, Mappin Street, S1 3JD Sheffield, UK

^dEindhoven University of Technology, Department of Mathematics and Computer Science, P.O. Box 513, 5600 MB Eindhoven, The Netherlands

Abstract

After 15 years of active research on the interaction between moving people and civil engineering structures, there is still a lack of reliable models and adequate design guidelines pertinent to vibration serviceability of footbridges due to multiple pedestrians. There are three key issues that a new generation of models should urgently address: pedestrian “intelligent” interaction with the surrounding people and environment, effect of human bodies on dynamic properties of unoccupied structure and inter-subject and intra-subject variability of pedestrian walking loads. This paper presents a modelling framework of human-structure interaction in the vertical direction which addresses all three issues. The framework comprises two main models: (1) a microscopic model of multiple pedestrian traffic that simulates time varying position and velocity of each individual pedestrian on the footbridge deck, and (2) a coupled dynamic model of a footbridge and multiple walking pedestrians. The footbridge is modelled as a SDOF system having the dynamic properties of the unoccupied structure. Each walking pedestrian in a group or crowd is modelled as a SDOF system with an adjacent stochastic vertical force that moves along the footbridge following the trajectory and the gait pattern simulated by the microscopic model of pedestrian traffic. Performance of the suggested modelling framework is illustrated by a series of simulated vibration responses of a virtual footbridge due to light, medium and dense pedestrian traffic. Moreover, the Weibull distribution is shown to fit well the probability density function of the local peaks in the acceleration response. Considering the inherent randomness of the crowd, this makes it possible to determine the probability of exceeding any given acceleration value of the occupied bridge.

Keywords: vibration engineering, human-induced vertical vibrations, pedestrian-structure interaction, footbridges, walking crowd loading

1. Introduction

In recent years, considerable advances have been made in the experimental characterisation and mathematical modelling of vertical pedestrian loads generated by individuals on stiff surfaces [1–3]. However, there is still a lack of fundamental data, reliable models and adequate design guidelines relevant to serviceability of light and slender footbridges that may vibrate perceptibly when occupied by multiple pedestrians. This study aims to advance the field by proposing a mathematical framework that describes a mechanism, generally known as “human-structure interaction”, by which multiple walking pedestrians interact with excessive vertical vibrations of the supporting structure. Modelling effect of multiple pedestrians walking on a lively structure should integrate the following three aspects:

A1) walking loading, so called “ground reaction forces” or “GRFs”, including their inter- and intra- subject variability [4];

*Corresponding author. Tel: (+39) 011.090.4844

Email addresses: fiammetta.venuti@polito.it (Fiammetta Venuti), vitomir.racic@polimi.it (Vitomir Racic), a.corbetta@tue.nl (Alessandro Corbetta)

11 A2) human-structure interaction (HSI), i.e. changes of dynamic properties of the empty structure due to the presence
12 of human bodies;

13 A3) modelling walking trajectories and gait patterns of the pedestrians under the influence of the surrounding people
14 and environment. In this paper, this aspect will be referred to as crowd dynamics even when describing different
15 group sizes.

16 Each of the aspects is discussed in the following paragraphs.

17 A1) GRFs are traditionally modelled as deterministic and perfectly periodic process presentable by a sum of
18 the first few dominant Fourier harmonics [1]. Nearly twenty years ago Kerr [5] acknowledged a great inter-subject
19 variability between amplitudes of individual footfall records. Further studies demonstrated inadequacy of the deter-
20 ministic modelling approach to describe reliably the actual random nature of individual walking excitation among the
21 human population [4, 6–9]. More recent research also showed that the Fourier modelling approach leads to signifi-
22 cant loss of information and introduction of inaccuracies during the data reduction process [2, 10–12]. For instance,
23 Brownjohn et al. [4] reported differences as high as 50% between simulated vertical vibrations due to the imperfect
24 (i.e. near-periodic) real walking forces and the corresponding periodic Fourier-based approximations. The error was
25 related to neglecting the energy around dominant harmonics in actual narrow band forces. Using the most compre-
26 hensive available database of continuously measured walking force time histories, Racic and Brownjohn [2] observed
27 significant differences in the level of “imperfection” for footfall timing and force amplitudes between individuals and
28 provided their very first mathematical model. Based on measured body kinematics of a group of five people crossing
29 a footbridge, van Nimmen et al. [12] showed that the variation in timing between successive footfalls is the key force
30 parameter in charge of getting a correct shape of simulated vibration response. Moreover, they speculated that the
31 apparent differences between measured and simulated vibration amplitudes could be attributed to the HSI.

32 A2) The HSI has intensively been studied in the lateral direction [1, 13, 14] since the infamous lateral vibration
33 problem of the London Millennium Bridge in 2000 [15]. It is now widely accepted that pedestrians are complex
34 and sensitive dynamic systems whose lateral motion and the corresponding contact forces are likely to be influenced
35 by the lateral sway of the supporting structure. Moreover, they often synchronise their footfalls with the lateral
36 structural motion (so called “lateral lock-in” effect), and by doing so they pump energy within the coupled human-
37 structure dynamic system while acting as negative dampers [15]. On the other hand, very little is known about HSI
38 in the vertical direction. Rare studies [12, 16–18] indicated that individuals mainly add damping to vertical structural
39 vibrations, but conclusive results are still not available. Bearing in mind the lack of viable research outcomes even
40 for a single pedestrian, it is not surprising that all relevant design guidelines still suggest models of vertical pedestrian
41 excitation based only on the GRFs as generated on rigid surfaces.

42 Two types of coupled pedestrian-structure models have been proposed so far to describe HSI in the vertical direc-
43 tion. Transferred and adopted from biomechanics of human gait, the first model represents a pedestrian as a simple
44 inverted pendulum that oscillates in the vertical plane while moving along a bridge. It was first used by Macdonald
45 [19] to simulate HSI on laterally swaying bridges, then adapted by Bocian et al. [17] to describe the vertical vibration.
46 In the latter study, a mechanism was identified by which the timing of the successive footfalls can be altered subtly on a
47 step-by-step basis without necessarily involving the lock-in with the vertical motion of the supporting structure. Their
48 numerical simulations showed that an individual pedestrian can act as a positive or a negative damper to the vertical
49 dynamic response, depending on the ratio between the bridge vibration frequency and pedestrian pacing frequency.
50 However, a pedestrian crowd on average add damping and mass.

51 The other type of HSI model couples a single-degree-of-freedom (SDOF) model of a structure and a moving
52 SDOF representing a pedestrian walking at a constant speed and pace rate. In Alexander’s model [20], vibration of
53 the coupled system is driven by a vertical harmonic force nested inside the pedestrian spring-mass-damper SDOF. The
54 force represents a source of the body energy materialised through the contraction of the leg muscles, which pushes
55 the upper body against the supporting structure. The model never gained widespread popularity since calibration
56 of the force parameters and dynamic properties of the pedestrian SDOF still remains a challenge due to the lack of
57 experimental data. As an alternative, Caprani et al. [21] used an external harmonic force attached to the base of the
58 pedestrian SDOF and applied to the structure only. While the force approximates walking GRFs measured on a stiff
59 surface, the role of the human SDOF is to alter dynamic properties of the occupied structure. Dang and Zivanovic
60 [22] carried out a series of vibration simulations with single pedestrians and reported equally good performance of

61 both models to simulate HSI in the vertical direction. Therefore, as the GRFs have already been measured, analysed
62 and modelled by the authors [2], the concept proposed by Caprani et al. has been adapted in the present study. Still,
63 there is considerable uncertainty about values of mass, stiffness and damping of the pedestrian SDOF which will be
64 discussed further in Section 2.

65 A3) All the above-mentioned models studied the case of a single pedestrian excitation, whereas a multi-pedestrian
66 traffic is a more likely load case scenario of footbridges. However, its modelling is much more challenging mainly due
67 to the shortage of knowledge on the proportion of individuals within a group or crowd who interact with each other, the
68 effect of the surrounding environment on pedestrian gait and walking trajectories, as well as the scale and character of
69 the resulting net dynamic loads on the structure. Pedestrians are “intelligent” agents who react to what they perceive
70 around them, with or without influence of the motion of the structure itself. There is strong evidence that peripheral
71 stimuli (e.g. visual, tactile and auditory) are an equally important factor influencing pedestrians walking [23–25].
72 Since the early sixties, applied mathematicians and transportation engineers have proposed several mathematical
73 models of the behaviour of pedestrians in crowds to address issues relevant to urbanism, evacuation of public buildings
74 and public safety. Moreover, they aimed to improve understanding of mass behaviour and the dynamics of self-
75 organizing pedestrian crowds (cf. e.g., [26, 27]). Depending on the scale of observation, the proposed models can be
76 divided into two main categories: (1) macroscopic models [28–30] based on the analogy between a flow of pedestrian
77 crowd and a continuous flow of a fluid, and (2) microscopic models [31–33] which consider a more detailed description
78 of the crowd using time varying positions and velocities of each individual. Both modelling approaches have been
79 used to simulate pedestrian crowd traffic only on footbridges that vibrate in the lateral direction (e.g. [34–37]). Despite
80 a large number of proposed models and their comparisons in the literature ([29, 38]), strong arguments in favour of one
81 modelling approach and its outstanding performance in the context of vibration engineering still cannot be found.
82 To the best understanding of the authors of the present study, macroscopic models imply a coarse approximation of
83 reality due to the “granular” nature of the crowd. Hence, their use can be more appropriate in cases of high pedestrian
84 density. Moreover, macroscopic models use average values of modelling parameters, such as mean crowd density and
85 velocity, thus are not able to account explicitly for the inter-subject variability of pedestrians. Therefore, microscopic
86 approach to modelling pedestrian traffic is adapted in this study.

87 This paper attempts to address all key aspects of the interaction between multiple pedestrians and a footbridge
88 that vibrates in the vertical direction. The research objective is to develop a robust framework which can be applied
89 to any kind of a lively footbridge with any kind of pedestrian traffic. For the sake of simplicity, in the present study
90 the framework is demonstrated on footbridges without obstacles along the deck (e.g. light posts and benches) and
91 occupied by unidirectional pedestrian traffic. A statistical approach to describe the inherent diversity of pedestrians
92 is applied whenever the relevant data was found available. The next section presents the modelling framework of
93 pedestrian-structure interaction adopted in this study. In Section 3, performance of the model is studied based on
94 simulated vibration response of four virtual footbridges due to different densities of pedestrian traffic. Finally, main
95 findings and conclusions are outlined in Section 4.

96 2. Description of the modelling framework

97 The flow chart in Figure 1 outlines the proposed modelling framework. It involves two different physical systems,
98 i.e. the pedestrians and the structure. The system “Pedestrians” is mathematically described by three sub-systems:
99 (C) a microscopic model of crowd dynamics (i.e., pedestrian traffic), (P) a mass-spring-damper SDOF model of each
100 individual pedestrian and (F) a stochastic force model of individual GRFs as proposed by Racic and Brownjohn [2].
101 The system “Structure” is modelled as a mass-spring-damper SDOF system (S). As highlighted in Figure 1, the three
102 sub-systems P, F and S describe the pedestrian-structure interaction (PSI) similar to the modelling approach proposed
103 by Caprani et al. [21]. Since there is no experimental evidence that the vertical structural vibration alters walking
104 velocity of pedestrians [17], it is assumed that the equations governing the crowd dynamics can be decoupled from
105 those simulating vibration response. The position along the bridge $\mathbf{x}_{p,i}$ and velocity $\mathbf{v}_{p,i}$ of the i -th pedestrian in a
106 group or crowd over time are generated first, then used as input data to the PSI model. Therefore, the coupling is only
107 between P and S systems.

108 The next three sections provide details of each sub-model.

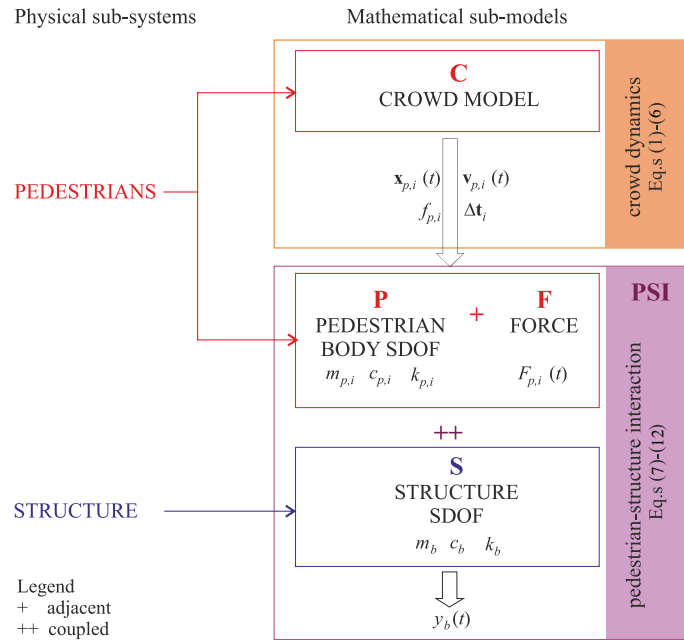


Figure 1: Outline of the modelling framework

2.1. Modelling crowd dynamics (C)

The crowd dynamics on the bridge deck is described from the microscopic perspective. Walking trajectory and gait of each individual in the crowd are defined by time varying vectors of the position \mathbf{x} and velocity \mathbf{v} of the body centre of mass. Modelling the walking trajectories is governed by the following principles [38]:

- each pedestrian enters the bridge at a preferred speed, so called *free speed*, and heads towards a target destination (i.e. the opposite end of the bridge) at so called *desired velocity*. These would be unchanged if his/her walking was undisturbed by the surrounding people and/or environment;
- while approaching the target, the desired velocity is modified on a step-by-step basis due to the interaction with neighbouring pedestrians and environment. This interaction happens within the so called *sensory region* [39], a portion of the space surrounding each pedestrian that affects his/her decision about when and where to place the next footfall. For the sake of simplicity but without a loss of generality, in this study the sensory region is limited only to the visual field of a pedestrian;
- interaction between pedestrians are anisotropic in space. This means that pedestrians react differently to what they perceive in front of them then beside and behind them. In this study, the interaction is restricted to a frontal sensory region;
- pedestrian interaction can be both repulsive and attractive. People normally tend to avoid crowded regions and collisions with other pedestrians, as well as to stay away from obstacles. They may also walk in smaller or larger groups, e.g. couples, which are entities that behave in a manner similar to single pedestrians [40]. In case of crowded situations, there is some evidence that pedestrians choose the fastest route to the bridge end rather than the shortest one [40], so having mainly the repulsive interaction with others that are on his/her way out [32]. Bearing all this in mind and for the sake of simplicity, the modelling framework is demonstrated only on cases of repulsive interaction in the present study.

A number of existing microscopic models based on the concept of “social force” [31, 41, 42] can account for the principles listed above. However, these models are commonly characterised by a far too large number of parameters,

133 which calibration would have been a challenge even if the adequate experimental data had been available. There-
 134 fore, a relatively simpler modelling concept originally proposed by Cristiani et al. [43] and applied to footbridges in
 135 [44] is adopted in this study to simulate a simple repulsive interaction. It provides a good balance between a suffi-
 136 ciently detailed description of the pedestrian behaviour and the number of input parameters, which will be discussed
 137 further in Section 3.1. While the general mathematical structure reported in [43] has been retained (see Eq.s (1) and
 138 (2)), the expressions of the velocities in the subsequent Eq.s (4) and (5) are an original contribution.

139 Let us consider a footbridge deck of dimensions $L \times B$, which lies in the horizontal plane $x - z$ (Figure 2a). For
 140 a crowd of N pedestrians, $\mathbf{x}_{p,i} = \{x_{p,i}, z_{p,i}\}$ is a vector of the position of the i -th pedestrian ($i=1, \dots, N$). His or her
 141 velocity, $\mathbf{v}_{p,i} = \{v_{xp,i}, v_{zp,i}\}$, is modelled as the sum of two distinct contributions: a desired velocity $\mathbf{v}_{d,i}$ and a social
 142 velocity $\mathbf{v}_{s,i}$ [38]:

$$\mathbf{v}_{p,i} = \frac{d\mathbf{x}_{p,i}}{dt} = \mathbf{v}_{d,i} + \sum_{\substack{j=1 \\ j \neq i}}^N \mathbf{v}_{s,i}(\mathbf{x}_{p,i}, \mathbf{x}_{p,j}). \quad (1)$$

143 The concept of desired velocity accounts for no interaction between an individual and the crowd. It assumes that each
 144 pedestrian is only aware of the surrounding environment and position of the target. It can be expressed as the vector
 145 sum of a *free desired velocity* $\mathbf{v}_{d,i}^f$ and *wall-repulsive velocity* $\mathbf{v}_{d,i}^w$:

$$\mathbf{v}_{d,i} = \mathbf{v}_{d,i}^f + \mathbf{v}_{d,i}^w. \quad (2)$$

146 The vector field of the free desired velocity depends on the geometry of the structure. In case of a narrow rectangular
 147 walkway ($L \gg B$) which is typical for a footbridge and unidirectional flow, it can be described as:

$$\mathbf{v}_{d,i}^f = v_i \{1, 0\}, \quad (3)$$

148 where v_i is the free speed (Figure 2a).

149 Wall-repulsive velocity $\mathbf{v}_{d,i}^w$ accounts for the boundary conditions imposed by the structural design, such as footbridge
 150 parapets and obstacles along the deck. It is directed perpendicular to the walls and is expressed as:

$$\mathbf{v}_{d,i}^w = \alpha \left[\frac{1}{(d_w(\mathbf{x}_{p,i}) - d_0)^\beta} - \frac{1}{(d_{w,0} - d_0)^\beta} \right] \mathbf{n}_w, \quad (4)$$

151 where $\mathbf{n}_w = \{0, \pm 1\}$ is the unit vector directed inwards the bridge longitudinal axis x , d_w is the distance between the
 152 pedestrian and the wall, d_0 is a half the lateral width of the human body, $d_{w,0}$ is the maximum distance from the wall
 153 at which the repulsion takes place, and α and β are the parameters that characterize the repulsion. Specifically, α
 154 is a scaling factor that controls the intensity of the repulsion, while β is the power, making the repulsion stronger in
 155 the proximity of the wall (Figure 2b). Therefore, pedestrians are laterally bounded within an effective width of the
 156 walkway $B_{eff} = B - 2d_0$.

157 The social velocity takes into account the interaction of the pedestrian i with the pedestrians who are within his/her
 158 sensory region (Figure 3b):

$$\mathbf{v}_{s,i} = -c \left[\frac{\mathbf{x}_{p,i} - \mathbf{x}_{p,j}}{|\mathbf{x}_{p,i} - \mathbf{x}_{p,j}|} \left(\frac{1}{|\mathbf{x}_{p,i} - \mathbf{x}_{p,j}|} - \frac{1}{R} \right) \right] \cdot h(\mathbf{x}_{p,i}, \mathbf{x}_{p,j}). \quad (5)$$

159 In Equation (5), the positive scalar c controls the intensity of the repulsive interaction, while h function limits the
 160 interaction to the sensory region. In this study, the sensory region is approximated as a circular sector area with radius
 161 R and angle $2\gamma \in [0, \pi]$ as illustrated in Figure 3a. The interaction function h is expressed by the following equation:

$$h(\mathbf{x}_{p,i}, \mathbf{x}_{p,j}) = \begin{cases} 1 & \text{if } |\mathbf{x}_{p,i} - \mathbf{x}_{p,j}| < R \ \& \ \frac{(\mathbf{x}_{p,i} - \mathbf{x}_{p,j}) \cdot \mathbf{v}_{d,i}}{|\mathbf{x}_{p,i} - \mathbf{x}_{p,j}| \cdot |\mathbf{v}_{d,i}|} > \cos \alpha \\ 0 & \text{elsewhere} \end{cases}. \quad (6)$$

162 Eq.s (4) and (5) can generate unnaturally high values of the velocity when a pedestrian is very close to the wall (Figure
 163 2b) or to another pedestrian (Figure 3b). On the other hand, the average upper value of walking velocity reported in
 164 the relevant literature is around 2.5 ms^{-1} (e.g., [45, 46]). Therefore, velocities generated through the crowd model are
 165 limited to 2.5 ms^{-1} .

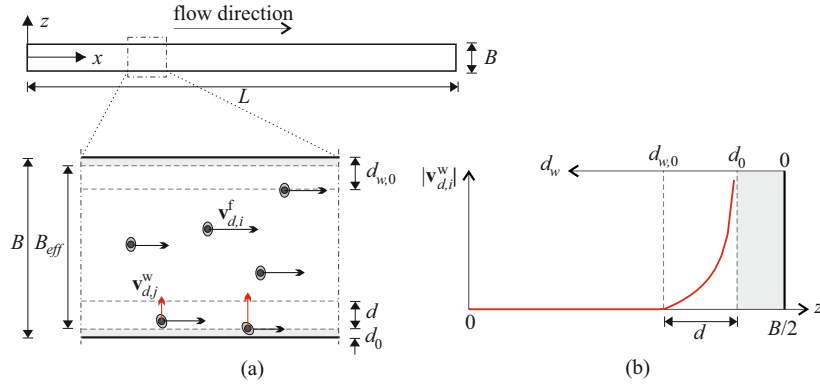


Figure 2: Scheme of (a) the footbridge deck and the desired velocity vectors; (b) qualitative trend of $v_{d,i}^w$ as a function of the distance d_w from the wall

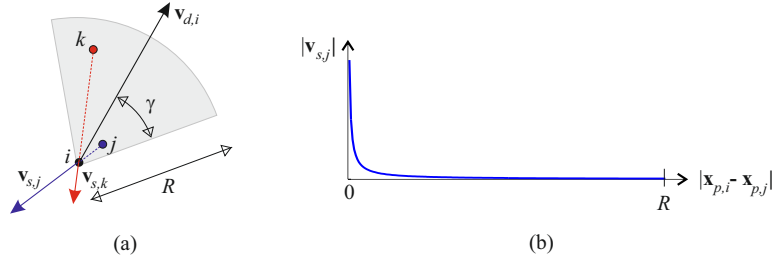


Figure 3: (a) Sensory region and illustration of velocity vectors and (b) qualitative trend of $v_{s,j}$ as a function of the distance between pedestrians i and j

2.2. Modelling pedestrian-structure interaction (PSI)

The PSI is described by a dynamic system that couples a SDOF representing a structural vibration mode of interest (S) and N SDOFs (P) with adjoining vertical walking GRFs (F) representing N individual pedestrians (Figure 4).

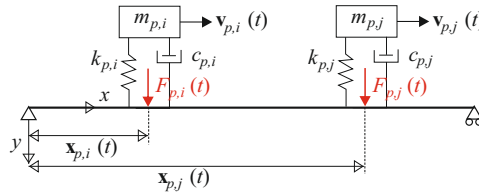


Figure 4: P-F representation of pedestrians walking along the footbridge

In the modal domain, the dynamics of the coupled system can be written in matrix form as:

$$\mathbf{M}\ddot{\mathbf{y}} + \mathbf{C}\dot{\mathbf{y}} + \mathbf{K}\mathbf{y} = \mathbf{F}, \quad (7)$$

where the mass, damping and stiffness matrices are:

$$\mathbf{M} = \begin{bmatrix} m_b & 0 & \cdots & 0 \\ 0 & m_{p,1} & \cdots & 0 \\ \vdots & \vdots & \ddots & \vdots \\ 0 & 0 & \cdots & m_{p,N} \end{bmatrix} \quad (8)$$

$$\mathbf{C} = \begin{bmatrix} c_b + \sum_{i=1}^N c_{p,i} \Phi^2(x_{p,i}(t)) & -c_{p,1} \Phi(x_{p,1}(t)) & \cdots & -c_{p,N} \Phi(x_{p,N}(t)) \\ -c_{p,1} \Phi(x_{p,1}(t)) & c_{p,1} & \cdots & 0 \\ \vdots & \vdots & \ddots & \vdots \\ -c_{p,N} \Phi(x_{p,N}(t)) & 0 & \cdots & c_{p,N} \end{bmatrix} \quad (9)$$

$$\mathbf{K} = \begin{bmatrix} k_b + \sum_{i=1}^N k_{p,i} \Phi^2(x_{p,i}(t)) & -k_{p,1} \Phi(x_{p,1}(t)) & \cdots & -k_{p,N} \Phi(x_{p,N}(t)) \\ -k_{p,1} \Phi(x_{p,1}(t)) & k_{p,1} & \cdots & 0 \\ \vdots & \vdots & \ddots & \vdots \\ -k_{p,N} \Phi(x_{p,N}(t)) & 0 & \cdots & k_{p,N} \end{bmatrix} \quad (10)$$

and the displacement and force vectors are:

$$\mathbf{y} = \begin{bmatrix} y_b \\ y_{p,1} \\ \vdots \\ y_{p,N} \end{bmatrix}, \quad \mathbf{F} = \begin{bmatrix} \sum_{i=1}^N F_{p,i} \Phi(x_{p,i}(t)) \\ 0 \\ \vdots \\ 0 \end{bmatrix} \quad (11)$$

Here m_b , c_b and k_b are the modal mass, damping and stiffness of the footbridge, while $m_{p,i}$, $c_{p,i}$, $k_{p,i}$ and $F_{p,i}(t)$ ($i = 1, \dots, N$) are modal mass, damping, stiffness and GRF of each individual. $y_b(t)$ and $y_{p,i}(t)$ are the displacement responses of the bridge at the antinode and the vertical displacements of each pedestrian oscillator respectively, while Φ is the unity-normalised mode shape of the structure.

Values of $m_{p,i}$, $c_{p,i}$ and $k_{p,i}$ are randomly assigned to different individuals using the statistics reported in Table 1. Pedestrian masses are generated using a Normal distribution as suggested in the literature (e.g., [47]), while uniform distributions are assumed for $c_{p,i}$ and $k_{p,i}$ due to the lack of extensive research on the statistics of these two body properties. Indeed, some rare results reported in the literature suggested different values for different activities, such as bouncing and running (see [21] for a review). The values across all reported activities are between 1000-100000 Nm^{-1} for stiffness and 0-1000 Nsm^{-1} for damping [18]. The range reported in [48] for $k_{p,i}$ is adopted in the present study. Damping level was decided after a comparison with the experimental research by Dougill et al. [49], who reported $\zeta_p = 25\%$ for bouncing people. Since damping for walking is expected to be lower than for bouncing [22], 400 Nsm^{-1} (corresponding to $\zeta_p = 25\%$ and the mean pedestrian mass and stiffness considered in the present study) was taken as the upper limit of the $c_{p,i}$ range (Table 1). Table 1 also reports ranges of the natural frequency and damping ratio corresponding to the adopted values of the pedestrian dynamic properties (calculated using $\text{mass}_{\text{mean}} \pm \text{mass}_{\text{std}}$). The adopted values are in line with the most recent study by Toso et al. [50].

Table 1: Dynamic properties of pedestrian bodies

Mass $m_{p,i}$ [kg] (mean, std)	75, 15
Damping $c_{p,i}$ [Nsm^{-1}] (min, max)	0, 400
Stiffness $k_{p,i}$ [Nm^{-1}] (min, max)	2000, 13000
Frequency [Hz] (min, max)	0.75, 2.34
Damping ratio ζ_p [-] (min, max)	0, 0.58

189

190 2.3. Modelling pedestrian GRFs (F)

191 Natural variability of the vertical walking loads for a single individual (i.e. intra-subject variability) and their
 192 randomness among the human population (i.e. inter-subject variability) is modelled using the stochastic generator of
 193 vertical walking force signals by Racic and Brownjohn [2]. The model is derived from a large database of individual
 194 vertical walking force records. Each synthetic force signal is unique as values of several key modelling parameters

195 are random numbers. The modelling parameters are stored in files which are classified in narrow frequency clusters
 196 distributed over a wide range of pacing rates approximately between 1-3 Hz. For a given pacing rate a set of modelling
 197 parameters can be selected randomly and equally likely from the corresponding cluster to synthesise an artificial force
 198 signal [2]. As the border frequencies are already unnaturally low or high and the major difference between the
 199 measured forces outside the range is only in the pacing rate [1], artificial forces at even lower or higher rates can be
 200 generated using the modelling parameters selected from the corresponding boundary clusters, i.e. around 1 Hz and
 201 around 3 Hz.

202 The key input parameters of the model relevant to this study are mean footfall rate $f_{p,\text{mean}}$ during footbridge
 203 crossing and durations of successive footfalls Δt . Both parameters are derived having information about pedestrian
 204 position $\mathbf{x}_{p,i}(t)$ and walking velocity $\mathbf{v}_{p,i}(t)$ from the simulations of the crowd dynamics presented in Section 2.1.
 205 Starting from the well-known relation between walking velocity v_p , step frequency f_p and step length l_p ($v_p = f_p l_p$),
 206 the vector of footfall timing $\Delta \mathbf{t} = [\Delta t^1, \Delta t^2, \dots, \Delta t^n]$ (where n is the number of steps) and the mean pacing rate $f_p =$
 207 $\text{mean}[f_p^0, f_p^1, \dots, f_p^n]$ of each pedestrian are derived according to the following algorithm (Figure 5):

208 Step 1: $x_p^0 = x_p(t = 0)$, $v_p^0 = v_p(t = 0)$ from crowd simulation;

209 $f_p^0 = f_p^0(v_p^0)$

210 $l_p^0 = v_p^0 / f_p^0$;

211 Step j : $x_p^j = x_p^{j-1} + l_p^{j-1}$;

212 $t^j = \text{time when } x_p(t) = x_p^j$;

213 $\Delta t^j = t^j - t^{j-1}$;

214 $v_p^j = v_p(t = t^j)$ from crowd simulation;

215 $f_p^j = f_p^{j-1} + (v_p^j - v_p^{j-1}) / (x_p^j - x_p^{j-1})$;

216 $l_p^j = v_p^j / f_p^j$.

217 The only missing data that cannot be directly derived from the crowd simulations is the value of the step frequency in
 218 Step 1. Here f_p^0 is determined as a function of the walking velocity according to the relationship [51], which is valid
 219 in the velocity range 0-2.5 ms^{-1} :

$$f_p = 2.93v_p - 1.59v_p^2 + 0.35v_p^3. \quad (12)$$

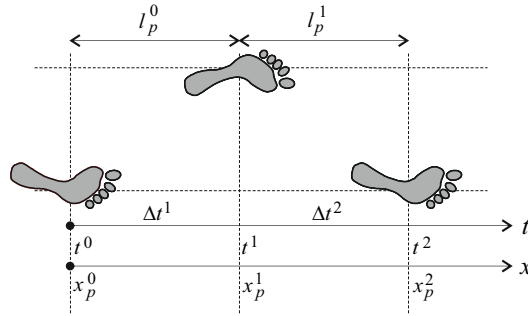


Figure 5: Pedestrian's position and timing of successive footfalls

220
 221 Figures 6a and b show an example of generated walking velocity and pacing rate on the step-by-step basis made
 222 by an individual pedestrian crossing the footbridge within a crowd, which density is 0.5 ped m^{-2} . The variability is the
 223 highest between 100-110s indicating that during this period the pedestrian interaction with other pedestrians and/or
 224 the bridge rails was the highest. The corresponding artificial force signal is shown in Figure 6c and d. While the
 225 variability of the force amplitudes is apparent in the time domain (Figure 6c), the variability of both amplitudes and
 226 footfall timing is evident in the frequency domain (Figure 6d). The dominant harmonics are at integer multiples of the
 227 mean step frequency 2.04 Hz, while the neighbouring harmonics are the result of the variability between successive
 228 footfalls.

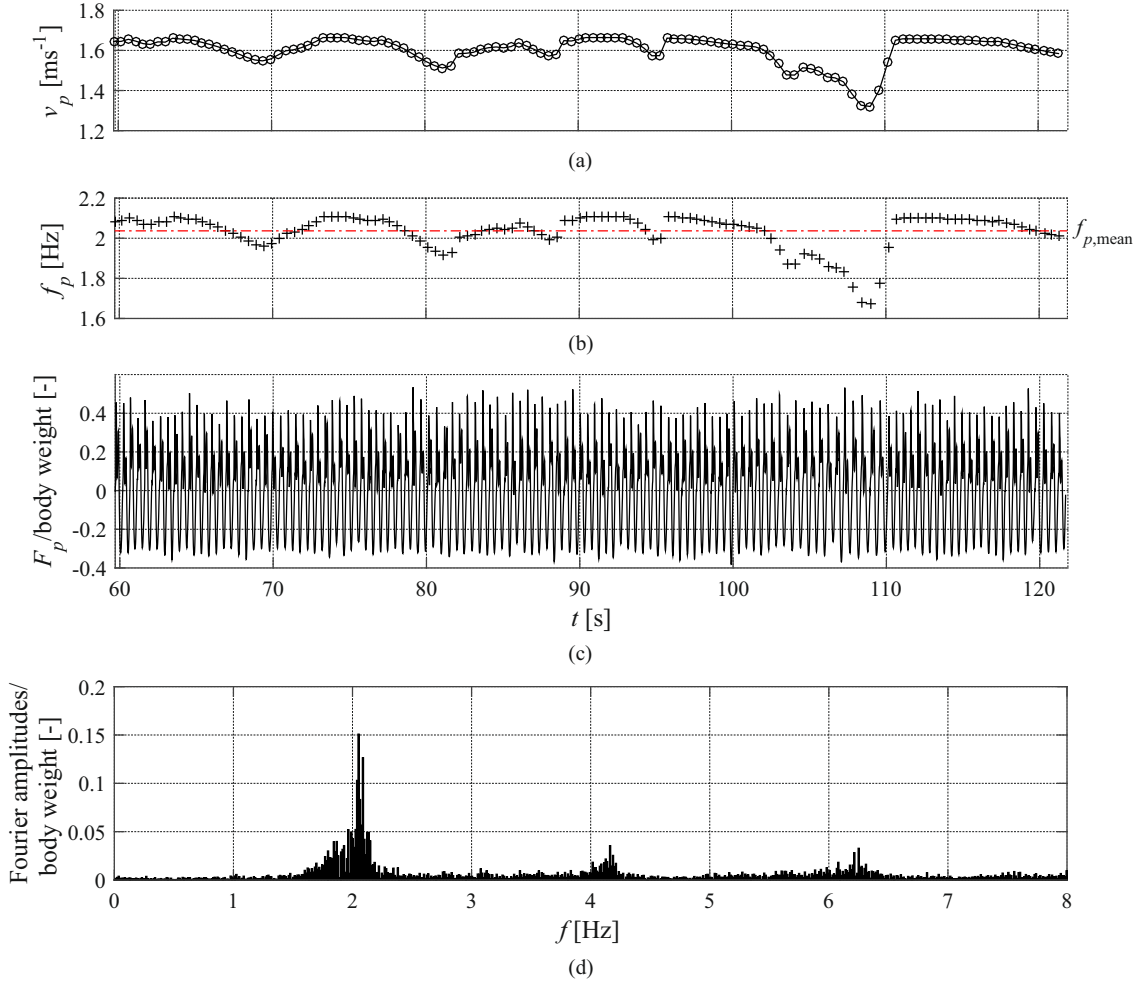


Figure 6: Walking velocity (a) and step frequency (b) on the step-by-step basis, the corresponding force time history (c) and its Fourier amplitude spectrum (d)

229 3. Evaluation of the model performance

230 This section aims to work out values of the crowd model parameters (Section 3.1) and to evaluate the performance
 231 of the proposed framework on four virtual footbridges with different dynamic properties due to different traffic sce-
 232 narios (Section 3.2). All the numerical simulations described in the following two sections are carried out using the
 233 same setup:

- 234 • the footbridge deck has length $L = 100$ m and width $B = 3$ m;
- 235 • a unidirectional and steady pedestrian flow is considered. The footbridge is initially empty. Arrival times of
 236 pedestrians are generated randomly using the Poisson distribution [52]. When a pedestrian leaves the footbridge,
 237 another pedestrian arrives from the opposite end, so the number of occupants is kept constant;
- 238 • lateral z coordinates of the arriving pedestrians across the bridge width are randomly assigned according to a
 239 uniform Probability Density Function (PDF) with boundaries $[B/2; B/2]$;
- 240 • values of the free speeds v_i are randomly assigned to each arriving pedestrian from a Normal PDF with mean
 241 v_m and standard deviation v_{std} (Table 2);

- duration of each simulation lasts three minutes. This time was chosen to allow multiple new arrivals on the footbridge, hence to increase a chance of observing all variations in the generated structural response due to the random nature of the occupants and their mutual interactions.

3.1. Values of the crowd model parameters

Calibration of input parameters in Eq.s (4)-(6) remains a challenge. This is mainly due to the lack of fundamental crowd data, especially recorded outside laboratory. Experimental data collection on real footbridges is still in its infancy due to the lack of adequate technology [53–57]. Luckily, reference values of d_0 , R , γ , v_m and v_{std} can be found in the literature (Table 2), coming from various application fields such as transportation engineering and biomechanics. In particular: d_0 is the mean value of half the lateral width of the human body after a comprehensive survey carried out for the worldwide population [58]; R is the maximum distance of visual attention, measured in busy shopping streets and public transport stations [59]; γ is the value commonly used in research of the human visual field [38, 60]; v_m and v_{std} are derived from an extensive study of walking velocity recorded in different countries and under various traffic conditions [61]. Values of the remaining four parameters α , β , $d = (d_{w,0} - d_0)$ and c can be determined by two sensitivity analyses presented in this section. They are designed to investigate how variation in values of each of the selected parameters affects crowd dynamics.

Table 2: Fixed values of selected parameters as featured in the literature

Parameter	d_0 [m]	R [m]	γ [°]	v_m [ms ⁻¹]	v_{std} [ms ⁻¹]
Value	0.225 [58]	2 [59]	85 [38, 60]	1.34 [61]	0.24 [61]

The parameters of the wall-repulsive velocity (Eq. 4) were studied first. A crowd of $N = 300$ pedestrians was selected to describe high density traffic of 1 pedm⁻², where interaction among the individuals is expected to have a strong impact on the crowd dynamics. Constant value of $c = 0.1$ m²s⁻¹ was adopted in all the simulations. Three sets of simulations, each relevant to either α , β or d and each repeated ten times, were performed in the first sensitivity analysis. In each set, values of two selected parameters were fixed, while value of the remaining parameter was varied within a selected range, as follows:

- A) Sensitivity to α : $\beta = 0.1$; $d = 0.35$ m (corresponds to half the lateral space needed by a pedestrian during walking, on average 62% higher than d_0 [58]); $\alpha = [20; 50; 100; 500; 1000]$ ms⁻¹m ^{β} ;
- B) Sensitivity to β : $\alpha = 20$ ms⁻¹m ^{β} ; $d = 0.35$ m; $\beta = [0.1; 0.5; 1; 5; 10; 50]$;
- C) Sensitivity to d : $\alpha = 20$ ms⁻¹m ^{β} ; $\beta = 5$; $d = [0.1; 0.225; 0.35; 0.475; 0.6]$ m.

10 simulations for each set was considered statistically reliable and also able to keep the overall simulation time under reasonable limits. The statistical reliability was checked by calculating mean and std of the crowd density at midspan ($45 < x < 55$ m) and averaging their values over increasing number of simulations $n = 1, 2, \dots, 50$. Figure 7 shows the relative error of both statistics between successive simulations $n - 1$ and n . When $n > 10$ the error is below 0.3% for the mean density and below 2% for the std, which could be considered sufficiently low for the purpose of this study.

For each of the three sets A, B and C, PDFs of the pedestrian positions along the footbridge width B are calculated for different values of the relevant parameter α , β and d , respectively, and averaged across the 10 simulations. Average PDFs are normalised to the maximum amplitude P_{max} in each set. Figure 8 shows the results. The values that yield the most uniform spread of the pedestrians across B were selected for the further analysis presented in Section 3.2. Broadly speaking, the results suggest:

- a general tendency of the pedestrians to walk at a distance $d_{w,0}$ from the bridge walls. This effect is due to the balance between two repulsive forces. On one hand, mutual repulsions bring pedestrians closer to the walls, while on another the wall repulsion force pedestrians away from the walls when they get as close as $d_{w,0}$;

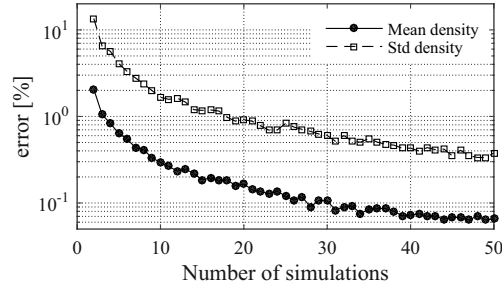


Figure 7: Error in the average mean and std crowd density for increasing number of simulations

- 281 • α is the least sensitive parameter (Figure 8a). Increasing its value of two orders of magnitude has a marginal
 282 effect on the crowd dynamics. Therefore, $\alpha = 20 \text{ ms}^{-1}\text{m}^\beta$, which corresponds to the lowest PDF peaks at
 283 distance $d_{w,0}$, was adopted in the simulations presented in the remaining part of the paper;
- 284 • there is a borderline value of β that yields two different distributions of the pedestrian positions along the width
 285 B (Figure 8b). For $\beta < 5$, pedestrians cluster in two rows that are $d_{w,0}$ far away from the left and the right
 286 edges (Figure 9a). On the other hand, for $\beta > 5$, distribution of the pedestrians is more uniform, with negligible
 287 difference between $\beta=5, 10$ or 50 (Figure 9b). $\beta=5$ is selected for the subsequent simulations as the lowest value
 288 that yields a significant reduction of the PDF peaks, i.e. a more uniform distribution of the pedestrians along
 289 the footbridge width;
- 290 • although different values of distance d shift the position of the PDF peaks (Figure 8c), the tendency of the
 291 pedestrians to walk at $d_{w,0}$ from the bridge walls remains unchanged. Therefore, $d = 0.35 \text{ m}$ is selected in the
 292 further simulations as it corresponds to the lowest PDF peaks and is the closest to the uniform distribution of
 293 pedestrians across the bridge width.

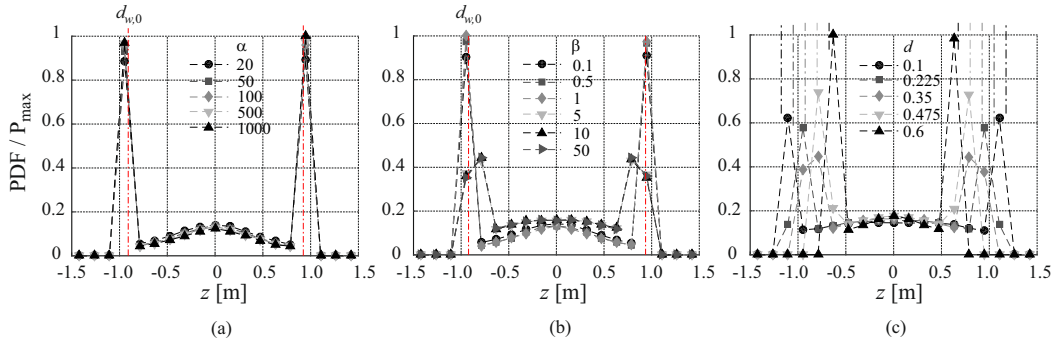


Figure 8: Normalised and averaged PDFs of pedestrian z coordinate for sets A (a), B (b) and C (c). Dash-dot lines refer to distance $d_{w,0}$ from the wall



Figure 9: Pedestrian positions at $t = 150 \text{ s}$ for case B, $\beta=0.1$ (a) and $\beta = 5$ (b)

294 The second sensitivity analysis tested only the effect of different values of the repulsion coefficient c on the crowd
 295 dynamics. 10 simulations for each combination of three different values of $c = [0.1; 0.2; 0.3] \text{ m}^2\text{s}^{-1}$ and five different
 296 crowd densities $\rho = [0.1; 0.3; 0.5; 0.8; 1] \text{ ped m}^{-2}$ were carried out. The last three values correspond to footbridge
 297 classes III, II and I from the Setra guideline [62], i.e. sparse, dense and very dense traffic, while the first two values are
 298 relevant to the case of unimpeded traffic. Mean and standard deviation of the pedestrian velocity when $N > 0.9\rho LB$
 299 were calculated for each simulation, then averaged over the 10 simulations for each combination of c and ρ . The
 300 results are plotted in Figure 10, together with the speed-density relation proposed by Weidmann in the so-called
 301 Kladek formula [58]:

$$v = 1.34 \left\{ 1 - \exp \left[-1.913 \left(\frac{1}{\rho} - \frac{1}{5.4} \right) \right] \right\}. \quad (13)$$

302 The model can simulate the decreasing trend in the speed-density relationship that is commonly reported in the lit-
 303 erature ([61] for a review). As the value of c increases, repulsion from other pedestrians becomes stronger and con-
 304 sequently their walking velocities decrease. Good match with the Kladek formula can be observed for all the values
 305 of c , though $c = 0.1 \text{ m}^2\text{s}^{-1}$ gives the best match in the considered density range (i.e. the black dots are the nearest to
 306 the Weidmann's curve). Figure 11 shows the empirical PDFs of the velocity obtained for $c = 0.1 \text{ m}^2\text{s}^{-1}$ and different
 307 crowd densities, as well as the Normal PDF set for the free velocity. The empirical PDFs maintain a bell-shaped
 distribution and are increasingly shifted towards lower velocity values as the number of pedestrians increases.

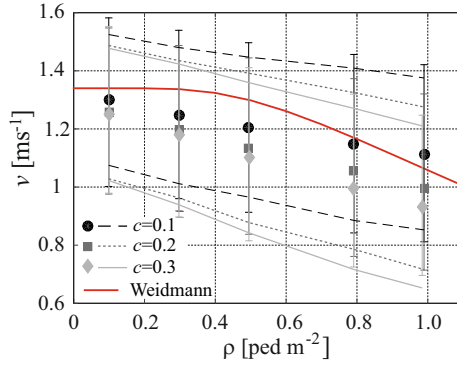


Figure 10: Velocity-density relationship calculated for different values of c . Dashed lines represent std values while the whiskers correspond to the 10th and 90th percentiles

308

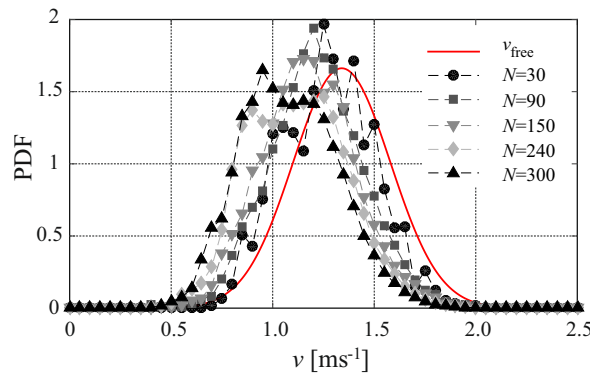


Figure 11: Empirical PDFs of the velocity corresponding to different N in comparison with the Normal PDF of the free velocity

309 Finally, values of parameters α , β , d and c adapted in simulations presented in the next section are summarised in
 310 Table 3.

Table 3: Suggested values of the free parameters in Eq.s (4) and (5)

Parameter	α [$\text{ms}^{-1}\text{m}^\beta$]	β [-]	d [m]	c [m^2s^{-1}]
Value	20	5	0.35	0.1

3.2. Vibration response of virtual footbridges

This section integrates everything presented so far to illustrate performance of the model on four virtual footbridges. Apart from the same dimensions (3x100 m), all bridges had common dynamic properties: natural frequency $f_b=2$ Hz, damping ratio $\zeta_b=0.5\%$ and a half-sine mode shape $\Phi = \sin(\pi x/L)$. The modal masses (and therefore stiffnesses) $m_b=[25000; 50000; 150000; 250000]$ kg were different to evaluate the effect of different bridge to pedestrian mass ratios on the structural dynamic response. The selected natural frequency of the bridge falls in the frequency range corresponding to the highest risk of resonance according to Setra guideline [62].

Three different traffic scenarios were studied on each virtual footbridge: $N=30$ pedestrians, corresponding to crowd density $\rho=0.1$ ped m^{-2} , $N=150$ pedestrians, corresponding to $\rho=0.5$ ped m^{-2} , and $N=300$ pedestrians, corresponding to $\rho=1$ ped m^{-2} . Since the described pedestrian-structure system has a higher degree of randomness than the crowd dynamics alone, a higher number of simulations than in Section 3.1 is expected to enable statistical reliability. Therefore, for each virtual bridge and each crowd scenario vibration response was simulated 50 times, as it was done in similar studies elsewhere [47].

To evaluate the influence of different sub-models of the framework on the structural response, for each combination of footbridge properties and crowd conditions the structural response was evaluated for following three cases:

PFS: pedestrian-structure interaction is taken into account, but the crowd dynamics is not considered. For the given crowd density ρ , the pedestrians enter the footbridge walking along straight lines and equally spaced at L/N . All the pedestrians walk at the same velocity $v(\rho)$, calculated by Eq.(13). The GRFs of all pedestrians have constant mean step frequency f_p calculated using Eq. (12) based on $v(\rho)$. The amplitudes of individual GRFs do not vary between successive steps, but they are different between individuals in the crowd. This is the only stochastic parameter kept in the numerical generator of artificial GRFs used in this case study [2].

CFS: pedestrian-structure interaction is neglected, i.e., pedestrians are modelled just as forces moving at the velocity obtained from the crowd model. As the velocity varies between successive steps for all pedestrians, the individual GRFs are stochastic in terms of both amplitudes and footfall timing and are different between individuals [2].

CPFS: all sub-models of the framework are included in their original form.

Computational simulations were carried out by adopting the same time step $dt=0.02$ s for both crowd and structure systems, in order to avoid resampling of the crowd results.

An example of a simulated acceleration time history and its Fourier amplitude spectrum for the three cases corresponding to 150 pedestrians (so $\rho=0.5$ ped m^{-2}) and $m_b=50$ tons are shown in Figure 12. In the PFS case (Figure 12a-b), the vibration response shows a clear peak that corresponds to the constant pedestrian pace rate 1.9 Hz. In the CFS case (Figure 12c-d), the crowd dynamics allows occasional synchronisation of pacing rates for a number of pedestrians yielding an occasional build-up of vibration response. Moreover, the resonance develops while their pacing rate matches the natural frequency of the structure. This can be observed on the portion of the acceleration time history in Figure 12c between approximately 75-85 s and 160-180 s. Therefore, the dominant harmonic in the Fourier amplitude spectrum corresponds to the footbridge natural frequency 2 Hz while the neighbouring harmonics are the result of the variability of the pedestrian footfall rates. How wide this spread would be depends on the level of variability of the pacing rates and damping of the structure. In the CPFS case (Figure 12e-f), the spectrum is much more dispersed as a result of the added effect of coupling between the footbridge and N pedestrian SDOFs [18], each having different dynamic properties (Table 1).

A large difference between the vibration responses corresponding to cases PFS and CFS clearly illustrates the importance of including crowd dynamics in simulations of the vibration response. Moreover, comparison between the

353 results relevant to CFS and CPFS cases illustrates equally strong effect of pedestrian-structure interaction. This obser-
 354 vation is also confirmed for different combinations of crowd density and bridge dynamic properties, as demonstrated
 in the following paragraphs.

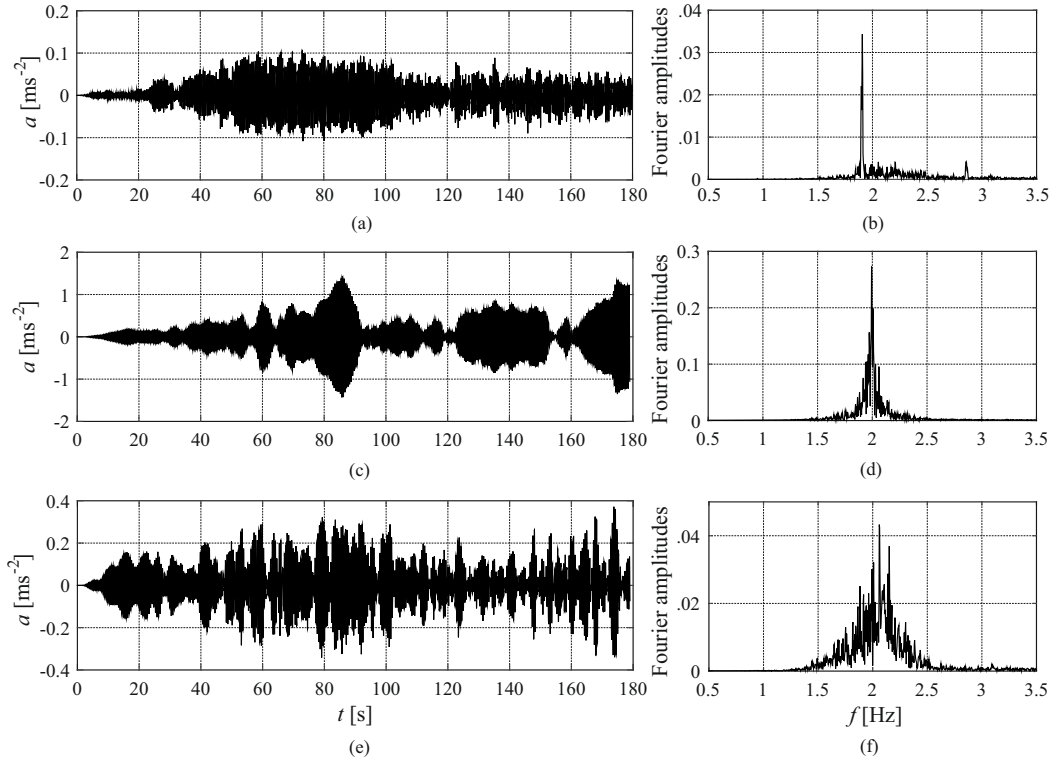


Figure 12: Time history and Fourier amplitudes of the acceleration responses for PFS (a)-(b), CFS (c)-(d) and CPFS (e)-(f) cases. $\rho=0.5 \text{ ped m}^{-2}$ and $m_b=50 \text{ tons}$

355 For each crowd scenario and virtual footbridge, peak accelerations and the maximum sliding 1s-RMS values [63]
 356 are extracted from the 50 simulated acceleration time histories. Both vibration measures are calculated using the total
 357 simulation time. Then, their mean values are computed across each set of the 50 simulations. The statistical reliability
 358 is evaluated by calculating the mean peak and 1s-RMS response averaged over increasing number of simulations.
 359 Figure 13 shows an example of relative error in average peak and 1s-RMS for increasing number of simulations
 360 ($n = 1, 2, \dots, 50$). Figure 13 refers to the set of simulations with $N=150$ pedestrians and $m_b=50$ tons. For both
 361 parameters the relative error falls below 1% for $n > 15$, while fluctuations are negligible for $n > 40$.

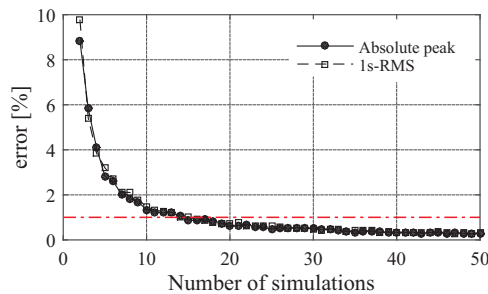


Figure 13: Error in average peak and 1s-RMS for increasing number of simulations ($N = 150$ pedestrians, $m_b = 50$ tons)

362 The influence of the crowd dynamics on the structural response can be observed by comparing the results obtained
 363 in the PFS and CPFS cases. The ratio a_r between the responses relevant to the two cases is shown in Figure 14 against
 364 the bridge to pedestrian mass ratio m_r , where:

$$a_r = \frac{a_{\text{PFS}}}{a_{\text{CPFS}}}, \quad m_r = \frac{m_b}{m_c} = \frac{m_b}{m_{p,\text{mean}} \rho B L / 2}. \quad (14)$$

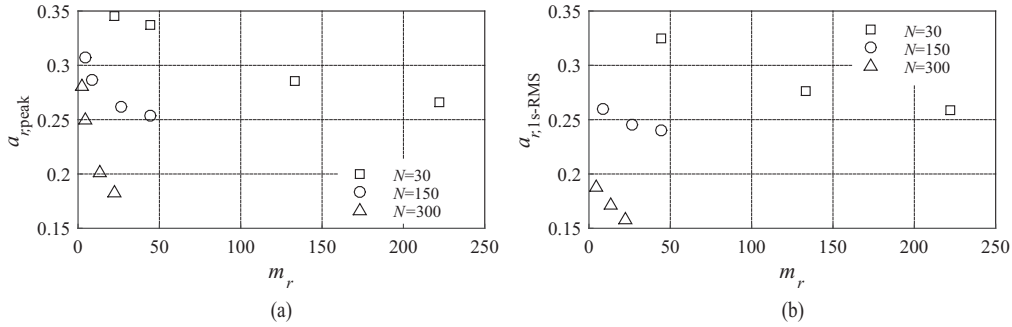


Figure 14: PFS-CPFS: ratio of the peak (a) and 1s-RMS (b) mean values of acceleration responses vs. m_r .

365
 366 Neglecting the crowd dynamics - i.e. the variability in the walking velocity and, consequently, in the pace rate of
 367 the pedestrians - the structural response is underestimated with respect to the CPFS case (Figure 14). This is because
 368 in the PFS case the step frequencies are the same for all the pedestrians and relatively far from the resonant frequency
 369 of the bridge ($f_p(N=30)=1.74$ Hz, $f_p(N=150)=1.9$ Hz, $f_p(N=300)=1.92$ Hz). On the other hand, in the CPFS
 370 case occasional synchronization of pace rate with the footbridge natural frequency may occur. Note that this result is
 371 dependent on the parameters chosen for the case study: $a_r > 1$ could be expected depending on the ratio f_p/f_b .

372 The significance of including PSI in the simulations of the vibration response is illustrated in Figure 15. It plots
 373 a_r ratio relevant to CFS and CPFS cases against m_r , where:

$$a_r = \frac{a_{\text{CFS}}}{a_{\text{CPFS}}}. \quad (15)$$

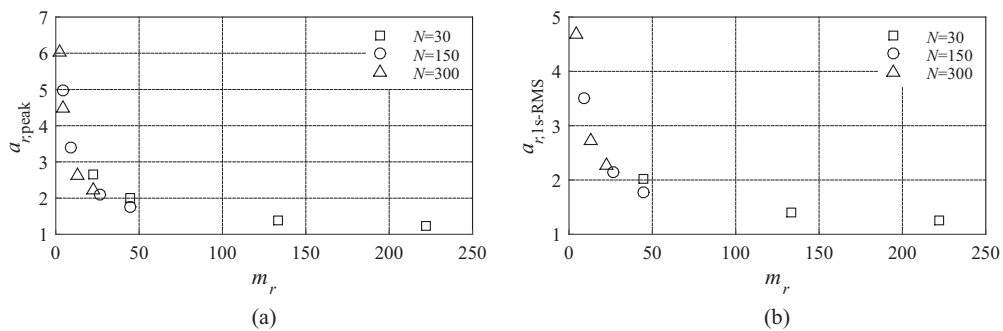


Figure 15: CFS-CPFS: ratio of the peak (a) and 1s-RMS (b) mean values of acceleration responses vs. m_r .

374
 375 The results show that the effect of PSI increases as the mass ratio approaches zero, e.g. when a very dense crowd
 376 crosses an extremely light footbridge. In such situations, the response relevant to CFS case is around 30 times higher
 377 than the corresponding CPFS case. This effect is due to the damping added by the pedestrian SDOFs and is in line
 378 with findings previously reported by others [17, 18].

379 The effect of pedestrian bodies on the coupled pedestrian-structure system can also be observed through a statisti-
 380 cal analysis of the CFS and CPFS results. Here, such analysis is demonstrated for the virtual footbridge with the mass
 381 50 tons. In all other cases, the analysis would follow the same steps.

382 Table 4 reports some statistics of the absolute peak response through 50 simulations for each crowd scenario.
 383 The selected statistics feature in the contemporary vibration serviceability guidelines of footbridges (e.g. [62, 64]).
 384 Moreover, the last column reports the maximum acceleration of the bridge calculated according to the most recent
 385 and widely used Setra guideline (SG) [62].

Table 4: Comparison between statistics of peak accelerations obtained through simulation results in the CFS and CPFS cases and maximum response calculated through SG ($m_b = 50$ tons)

N	CFS				CPFS				SG
	Mean	Std	Min-Max	95%ile	Mean	Std	Min-Max	95%ile	
30	0.8555	0.1728	0.4998-1.1847	1.1395	0.4266	0.0751	0.2823-0.5788	0.5392	1.4911
150	1.413	0.251	0.9829-2.2788	1.9441	0.4161	0.0714	0.2992-0.597	0.566	3.3342
300	1.7608	0.2784	1.201-2.4037	2.2545	0.3934	0.0505	0.3013-0.5389	0.4843	11.4226

386 SG load model is deterministic and recognises two crowd scenarios: sparse crowd for $\rho < 1$ ped m^{-2} and dense
 387 crowd for $\rho \geq 1$ ped m^{-2} . In both cases, the effective force is defined in terms of an “equivalent” number of perfectly
 388 synchronised pedestrians N_{eq} uniformly distributed along the bridge and walking in time with its vertical natural
 389 frequency:

$$\begin{aligned} N_{eq} &= 10.8 \sqrt{\zeta N} && \text{for } \rho < 1 \text{ ped } m^{-2} \\ N_{eq} &= 1.85 \sqrt{N} && \text{for } \rho \geq 1 \text{ ped } m^{-2} \end{aligned} \quad (16)$$

390 The values of N_{eq} were determined from simulations of the acceleration response of a bridge to increasing numbers
 391 of pedestrians crossing the bridge. For the “dense crowd” the pedestrian pacing frequency was equal to the natural
 392 frequency of the bridge. For other densities the frequency was selected randomly around the natural frequency. The
 393 phase of each pedestrian’s pacing was uniformly distributed randomly over the cycle. The “equivalent” number of
 394 pedestrians is best fit to the number required to produce the 95th percentile (95%ile) highest acceleration response of
 395 the random pacing pedestrian simulations. The amplitude of the equivalent load per square metre is defined as:

$$q_{eq} = \frac{N_{eq}}{LB} F_v \Psi_v, \quad (17)$$

396 where $F_v = 280$ N and $\Psi_v = 1$ for $1.7 < f_b < 2.1$ Hz. In the present study, the sparse crowd model features $N=30$
 397 and $N=150$ pedestrians, while the actual size of the dense crowd model is $N=300$ pedestrians. The peak acceleration,
 398 which represents the 95%ile of the peak response due to random pedestrians, is then calculated as:

$$a_{\text{peak}} = \frac{1}{2\zeta_b} \frac{q_{eq} B \int_0^L \Phi(x) dx}{m_b}. \quad (18)$$

399 The results summarised in Table 4 point to the following conclusions:

- 400 • when PSI is not considered (CFS), all the vibration measures show the same increasing trend as SG for increas-
 401 ing number of pedestrians. Values of the 95%ile of the peak response are of the same order of magnitude as
 402 SG for the sparse crowd ($N=30$ and 150), while for the dense crowd ($N=300$) the response calculated through
 403 SG is much higher. This is because the SG load model for a dense crowd is based on the assumption that all
 404 pedestrians walk at the same step frequency, while the presented crowd model does not explicitly account for
 405 the possibility of synchronization among the pedestrians;
- 406 • when PSI is considered (CPFS), the 95%ile peak response is up to 6 times lower than SG for sparse crowd and
 407 almost 23 times lower in the case of dense crowd. Moreover, the vibration measures do not show an increasing
 408 trend for increasing N . This is due to the additional damping of the pedestrians. Hence, the importance of
 409 taking into account PSI is demonstrated again.

410 The added damping due to pedestrian bodies can be better understood by studying time changes of the effective
 411 damping ratio of the coupled system ζ in the CPFS case:

$$\zeta = \frac{c_{1,1}}{2\sqrt{(m_b k_b)}}. \quad (19)$$

412 Here, $c_{1,1}$ is the first diagonal term of the damping matrix \mathbf{C} .

413 Figure 16 illustrates an example of a simulation with 150 pedestrians and $m_b=50$ tons and the adopted parameters
 414 of the pedestrian SDOF (the same as in Figure 12e-f). The figure also shows the number of pedestrians on the
 415 footbridge as the simulation progresses. As expected, the damping ratio increases rapidly during approximately first
 416 80 s while the pedestrians gradually occupy the full length of the footbridge, i.e. until the occupancy has approached
 417 the peak of $N=150$ pedestrians. In the remaining part of the simulation, the value of ζ varies slightly although the
 418 number of pedestrians is constant. This is due to the varying positions of the pedestrian SDOFs as they move along
 the footbridge deck, thus are exposed to different ordinates of the structural mode shape.

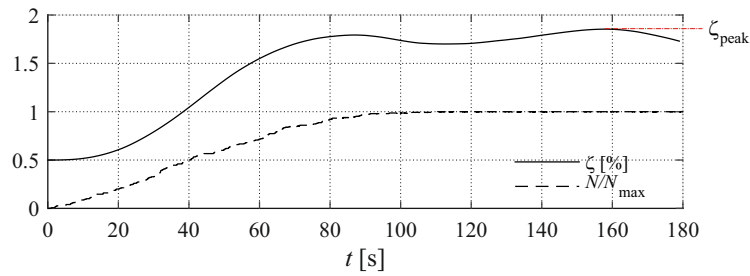


Figure 16: Example of time history of the effective damping ratio and of the number of pedestrians on the footbridge for $N = 150$ and $m_b = 50$ tons

419 The peak value of the effective damping ζ_{peak} was found for each simulated vibration response, then the mean peak
 420 value is calculated across the 50 simulations for each crowd scenario and each virtual footbridge. Mean peak values
 421 were normalised by the damping of the empty structure ζ_b and plotted in Figure 17a against m_r . The figure shows a
 422 decreasing trend of $\zeta_{r,\text{peak}}$ as m_r increases, which is similar to the trend of $a_{r,\text{peak}}$ observed in Figure 15. Experimentally
 423 estimated values of the effective damping found in the literature are also reported in Figure 17 for comparison. The
 424 values by Zivanovic et al. [16] were extracted from measured acceleration responses of a laboratory footbridge
 425 structure at the University of Sheffield due to groups of two to 10 people walking. The data of Salyards and Hua
 426 [65] correspond to studies with groups of one to 19 people standing with bent knees on a laboratory floor structure.
 427 The values obtained from the numerical simulations carried out in this study are in line with those experimentally
 428 measured.

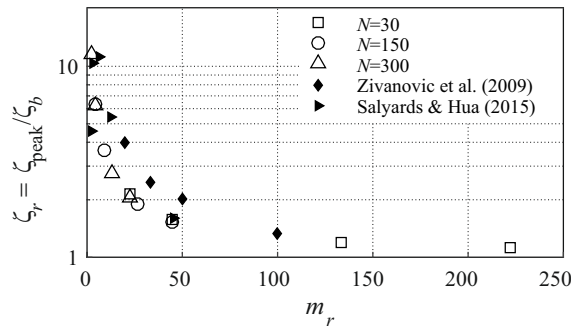


Figure 17: Mean peak damping ratio ζ_r against m_r

429 Finally, the acceleration response in the CPFS case is analysed in a detail considering the case of $N=150$ pedes-
 430 trians and $m_b=50$ tons. Figure 18a shows the empirical PDF of the acceleration considering all the 50 simulated time
 431

432 histories, together with the fitted Normal distribution. It can be observed that the empirical PDF does not closely
 433 follow the Normal distribution. Zivanovic [47] observed a similar trend in a 44-minute-long vertical acceleration
 434 response recorded on the Podgorica footbridge due to a regular pedestrian traffic. As a result, the peak per cycle
 435 accelerations do not follow the Rayleigh distribution [66], which is apparent in Figure 18b. As in Zivanovic [47],
 436 the Weibull distribution also provides the best fit to the empirical PDF in the present study. This is more evident by
 437 looking at the CDF of the peak per cycle response (Figure 19a) and the corresponding probability plot (Figure 19b).
 The latter shows that the curve relative to Weibull distribution almost match the diagonal line.

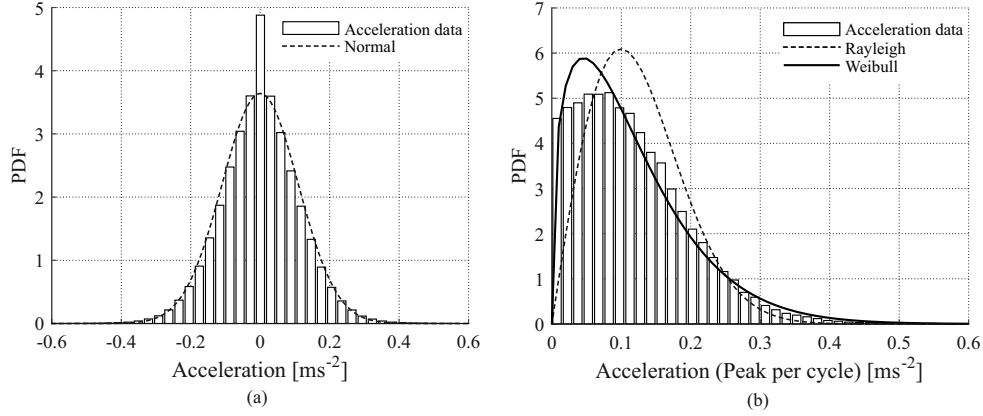


Figure 18: PDFs of the instantaneous (a) and the peak per cycle (b) acceleration

438

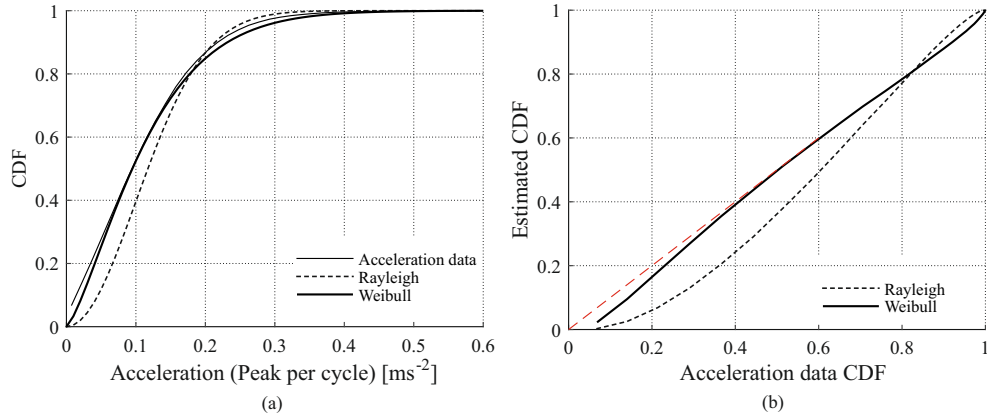


Figure 19: CDF of the peak per cycle acceleration (a) and probability plot (b)

439 The fitted Weibull distribution can be used to estimate the likelihood of exceeding any given acceleration limit. In
 440 the same way Carroll et al. [36] processed the results from the study of the lateral bridge vibrations, but their lateral
 441 acceleration data clearly followed the Rayleigh distribution. The most likely peak acceleration value (extreme peak)
 442 $A_{E,peak}$ occurring during the return period T_r can be estimated through the following equation:

$$A_{E,peak} = \lambda \left[-\ln \left(\frac{1}{n} \right) \right]^{1/\kappa}, \quad (20)$$

443 where λ and κ are respectively the scale and shape parameters of the Weibull distribution, $n = T_r \cdot f_m$ is the number of
 444 peaks in the return period and f_m is the maximum frequency of oscillation. Moreover, the peak with a 5% probability

445 of exceedance $A_{E,95}$ in the return period can be calculated as:

$$A_{E,95} = \lambda \left[-\ln(1 - 0.95^{1/n}) \right]^{1/\kappa}. \quad (21)$$

446 Figure 20 shows $A_{E,peak}$ and $A_{E,95}$ as a function of T_r and assuming $f_m=2$ Hz. For instance, if a return period of 2
 447 hours is considered as representative of peak morning/evening usage periods, from the limited data in this study the
 448 most likely peak acceleration is 0.67 ms^{-2} and the peak acceleration with 5% probability of exceedance is 0.82 ms^{-2} .
 Both values seem realistic and possible considering the crowd size and properties of the selected virtual bridge.

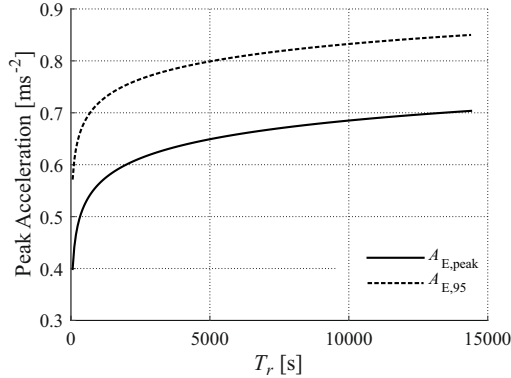


Figure 20: Peak acceleration as a function of the return period T_r

449

450 4. Conclusions

451 This study presents a mathematical framework to simulate vibration response of footbridges that are prone to
 452 excessive vertical vibrations due to multiple pedestrians walking. The framework puts together two key elements
 453 that are necessary to describe the phenomenon: (1) a model of the crowd dynamics, which describes the “intelligent”
 454 pedestrian behaviour through the mutual interaction between individuals in a group or crowd as well as with the
 455 environmental constrains; (2) a model of the pedestrian-structure interaction (PSI), which takes into account intra-
 456 and inter-subject variability of individual walking loading and dynamic interaction between pedestrian bodies and the
 457 occupied structure.

458 A microscopic crowd model was selected to describe pedestrian trajectories and walking velocities in time and
 459 space. PSI was modelled by coupling a SDOF system describing the structure and N SDOFs describing a group/crowd
 460 of N pedestrians. The pedestrian SDOFs move along the structure following the walking paths and velocities simulated
 461 by the microscopic model of the crowd dynamics and thereby alter the dynamic properties of the empty structure due
 462 to the presence of walking human bodies. Moreover, each pedestrian SDOF is accompanied by a walking force time
 463 history generated by a stochastic model of realistic walking force signals available in the literature. The parameters of
 464 the crowd model were estimated for different pedestrian traffic scenarios using two sensitivity studies. Values of the
 465 mass, spring and damping of the pedestrian SDOFs are adapted from the previously published studies.

466 A sound performance of the proposed modelling framework was illustrated by a series of simulated vibration
 467 responses of four virtual footbridges under light, medium and dense pedestrian traffic. Moreover, comparison between
 468 the results corresponding to cases with and without considering PSI allowed estimating the effective damping of the
 469 pedestrian-structure system. The damping added by the pedestrians can reach values as high as 5% depending on the
 470 bridge to pedestrian mass ratio. The obtained results are in line with the findings from other published studies that
 471 took completely different approaches to modelling PSI.

472 The simulated acceleration data were further studied following a statistical approach suggested by Zivanovic
 473 [47] and Carroll et al. [36]. Carroll’s lateral acceleration samples followed the Normal distribution, so the local
 474 peaks followed the Raleigh distribution by default. In the present study of the vertical acceleration data, the Weibull

475 distribution fitted best PDF of the peaks. This is in line with the findings by Zivanovic [47] who processed long-
476 term vertical acceleration data measured on a real footbridge under a regular pedestrian traffic. Whatever the correct
477 distribution is, having an estimate of daily traffic conditions and knowing properties of the occupied bridge, it is
478 possible to determine the probability of exceeding any given acceleration value. Considering the inherent randomness
479 in crowd dynamics, human bodies and the loading, such an approach is better suited for vibration serviceability
480 assessment of pedestrian structures than a single acceleration value featuring in the relevant design guideline, such as
481 Setra. Moreover, the statistical treatment is perfectly suited for performance-based vibration serviceability assessment,
482 which still needs to be codified.

483 The proposed modelling framework provides a solid foundation for its more refined versions in the future. Each
484 of its sub-models in the current version is adapted or derived from the most reliable models and data known to the
485 authors. The sub-models describing crowd dynamics, pedestrian moving body and walking forces can be updated
486 independently as soon as their better models have been published or the relevant experimental data have been made
487 available for calibration and verification.

488 Acknowledgements

489 The authors would like to acknowledge the financial support provided by the UK Engineering and Physical Sci-
490 ences Research Council (EPSRC) for grants reference EP/I029567/1 “Synchronisation in dynamic loading due to
491 multiple pedestrians and occupants of vibration-sensitive structures” and EP/K03877X/1 “Modelling complex and
492 partially identified engineering problems - application to the individualised multiscale simulation of the musculoskele-
493 tal system”. The study has been also granted by the ISI Foundation - CRT Foundation within the Lagrange project
494 “Multi-scale modeling of complex crowd-structure interaction for applications in Civil Engineering”.

495 References

- 496 [1] V. Racic, A. Pavic, J. M. W. Brownjohn, Experimental identification and analytical modelling of human walking forces: Literature review,
497 *Journal of Sound and Vibration* 326 (2009) 1–49.
- 498 [2] V. Racic, J. M. W. Brownjohn, Stochastic model of near-periodic vertical loads due to human walking, *Advanced Engineering Informatics* 25
499 (2011) 259 – 275.
- 500 [3] V. Racic, J. B. Morin, Data-driven modelling of dynamic excitation of bridges induced by people running, *Mechanical Systems and Signal*
501 *Processing* 43 (2014) 153–170.
- 502 [4] J. Brownjohn, A. Pavic, P. Omenzetter, A spectral density approach for modelling continuous vertical forces on pedestrian structures due to
503 walking, *Canadian Journal of Civil Engineering* 158 (2004) 65–77.
- 504 [5] S. Kerr, Human-induced loading on staircases, Ph.D. thesis, University of London (UK), Department of Mechanical Engineering (1998).
- 505 [6] S. Živanović, A. Pavic, P. Reynolds, Human-structure dynamic interaction in footbridges, *Bridge Engineering* 158 (BE4) (2005) 165–177.
- 506 [7] C. Sahnaci, M. Kasperki, Random loads induced by walking, in: *Proceedings 6th International Conference on Structural Dynamics EURO-*
507 *DYN 2005*, Paris, France, 2005.
- 508 [8] S. Živanović, A. Pavic, Quantification of dynamic excitation potential of pedestrian population crossing footbridges, *Shock and Vibration* 18
509 (2011) 563–577.
- 510 [9] H. Dang, S. Živanović, Experimental characterisation of walking locomotion on rigid level surfaces using motion capture system, *Engineering*
511 *Structures* 91 (2015) 141–154.
- 512 [10] C. Middleton, J. Brownjohn, Response of high frequency floors: a literature review, *Engineering Structures* 32 (2) (2009) 337–352.
- 513 [11] V. Racic, J. M. W. Brownjohn, Mathematical modelling of random narrow band lateral excitation of footbridges due to pedestrians walking,
514 *Computers & Structures* 90-91 (2012) 116–130.
- 515 [12] K. Van Nimmen, G. Lombaert, I. Jonkers, G. D. Roeck, P. Van den Broek, Characterisation of walking loads by 3d inertial motion tracking,
516 *Journal of Sound and Vibration* 333 (20) (2014) 5212 – 5226.
- 517 [13] F. Venuti, L. Bruno, Crowd-structure interaction in lively footbridges under synchronous lateral excitation: A literature review, *Physics of*
518 *Life Reviews* 6 (3) (2009) 176–206.
- 519 [14] E. Ingolfsson, C. Georgakis, J. Jonsson, Pedestrian-induced lateral vibrations of footbridges: A literature review, *Engineering Structures* 45
520 (2012) 21–52.
- 521 [15] P. Dallard, T. Fitzpatrick, A. Flint, A. Law, R. M. Ridsdill Smith, M. Willford, M. Roche, The London Millennium Bridge: pedestrian-induced
522 lateral vibration, *Journal of bridge Engineering* 6 (6) (2001) 412–417.
- 523 [16] S. Živanović, I. Diaz, A. Pavic, Influence of walking and standing crowds on structural dynamic properties, in: *Proceedings IMAC XXVII*,
524 Orlando, Florida USA, 2009.
- 525 [17] M. Bocian, J. Macdonald, J. Burn, Biomechanically-inspired modelling of pedestrian-induced vertical self-excited forces, *ASCE Journal of*
526 *Bridge Engineering* 18 (12) (2012) 1336–1346.
- 527 [18] E. Shahabpoor, A. Pavic, V. Racic, Modelling effect of pedestrians walking on dynamic properties of structures, in: *Proceedings of IMAC*
528 *XXXI: A Conference and Exposition on Structural Dynamics*, Orange County, California, USA, 2013.

- 529 [19] J. Macdonald, Lateral excitation of bridges by balancing pedestrians, *Proceedings of the Royal Society A Mathematical, Physical and*
530 *Engineering Sciences* 465 (2009) 10551073.
- 531 [20] N. Alexander, Theoretical treatment of crowd-structure interaction dynamics, *Structures and Buildings* 159 (2006) 329–338.
- 532 [21] C. Caprani, J. Keogh, P. Archbold, P. Fanning, Characteristic vertical response of a footbridge due to crowd loading, in: *Proceedings of the*
533 *8th International Conference on Structural Dynamics EURODYN 2011*, Leuven, Belgium, 2011.
- 534 [22] H. Dang, S. Živanović, Modelling pedestrian interaction with perceptibly vibrating footbridges, *FME Transactions* 41 (2013) 271–278.
- 535 [23] A. E. Patla, Understanding the roles of vision in the control of human locomotion, *Gait & Posture* 5 (1997) 54–69.
- 536 [24] J. J. Gibson, *The perception of the visual world*, The Riverside Press, Boston, 1950.
- 537 [25] S. M. Kosslyn, Measuring the visual angle of the mind’s eye, *Cognitive Psychology* 10 (1978) 356–389.
- 538 [26] M. Moussaïd, D. Helbing, S. Garnier, A. Johansson, M. Combe, G. Theraulaz, Experimental study of the behavioural mechanisms underlying
539 self-organization in human crowds, *Proceedings of the Royal Society B: Biological Sciences* (2009) rspb–2009.
- 540 [27] M. Moussaïd, E. G. Guilloit, M. Moreau, J. Fehrenbach, O. Chabiron, S. Lemerrier, J. Pettré, C. Appert-Rolland, P. Degond, G. Theraulaz,
541 *Traffic instabilities in self-organized pedestrian crowds*, *PLoS computational biology* 8 (3) (2012) e1002442.
- 542 [28] R. L. Hughes, A continuum theory for the flow of pedestrians, *Transportation Research Part B* 36 (2002) 507–535.
- 543 [29] N. Bellomo, C. Dogbé, On the modelling crowd dynamics from scaling to hyperbolic macroscopic models, *Mathematical Models and Meth-*
544 *ods in Applied Sciences* 18 (2008) 1317–1346.
- 545 [30] V. Coscia, C. Canavesio, First order macroscopic modelling of human crowds, *Mathematical Models and Methods in Applied Sciences*
546 *18 (Supplement)* (2008) 1217–1247.
- 547 [31] D. Helbing, P. Molnár, Social force model for pedestrian dynamics, *Physical Review E* 51 (5) (1995) 4282–4286.
- 548 [32] D. Helbing, P. Molnár, I. J. Farkas, K. Bolay, Self-organizing pedestrian movement, *Environment and Planning B: Planning and Design* 28 (3)
549 (2001) 361–383.
- 550 [33] S. P. Hoogendoorn, P. H. L. Bovy, Simulation of pedestrian flows by optimal control and differential games, *Optimal Control Applications*
551 *and Methods* 24 (2003) 153–172.
- 552 [34] F. Venuti, L. Bruno, The synchronous lateral excitation phenomenon: modelling framework and application, *Comptes Rendus Mecanique*
553 *335 (2007)* 739–745.
- 554 [35] L. Bruno, F. Venuti, Crowd-structure interaction in footbridges: modelling, application to a real case-study and sensitivity analyses, *Journal*
555 *of Sound and Vibration* 323 (2009) 475–493.
- 556 [36] S. P. Carroll, J. S. Owen, M. F. M. Hussein, Modelling crowd-bridge dynamic interaction with a discretely defined crowd, *Journal of Sound*
557 *and Vibration* 331 (2012) 2685–2709.
- 558 [37] S. P. Carroll, J. S. Owen, M. F. M. Hussein, A coupled biomechanical/discrete element crowd model of crowd-bridge dynamic interaction
559 and application to the Clifton Suspension Bridge, *Engineering Structures* 49 (2013) 58–75.
- 560 [38] E. Cristiani, B. Piccoli, A. Tosin, *Multiscale Modeling of Pedestrian Dynamics*, Vol. 12 of MS&A: Modeling, Simulation and Applications,
561 Springer International Publishing, 2014.
- 562 [39] J. J. Fruin, *Pedestrian planning and design*, Elevator World Inc., 1987.
- 563 [40] J. Ganem, A behavioral demonstration of fermat’s principle, *The Physics Teacher* 36 (1998) 76–78.
- 564 [41] F. Zanlungo, T. Ikeda, T. Kanda, Social force model with explicit collision prediction, *Europhysics Letters* 93 (6) (2011) 68005.
- 565 [42] M. Chraïbi, A. Seyfried, A. Schadschneider, Generalized centrifugal-force model for pedestrian dynamics, *Physical Review E* 82 (4) (2010)
566 046111.
- 567 [43] E. Cristiani, B. Piccoli, A. Tosin, Multiscale modeling of granular flows with application to crowd dynamics, *Multiscale Modeling and*
568 *Simulation* 9 (1) (2011) 155–182.
- 569 [44] L. Bruno, A. Corbetta, A. Tosin, From individual behaviour to an evaluation of the collective evolution of crowds along footbridges, *Journal*
570 *of Engineering Mathematics* DOI 10.1007/s10665-016-9852-z, to appear.
- 571 [45] H. Bachmann, W. Ammann, *Vibration in structures induced by man and machines*, in: *Structural Engineering Documents*, Vol. 3a, IABSE,
572 Zurich, 1987.
- 573 [46] J. E. Bertram, A. Ruina, Multiple walking speed-frequency relations are predicted by constrained optimization, *Journal of Theoretical Biology*
574 *209 (2001)* 445–453.
- 575 [47] S. Živanović, Benchmark footbridge for vibration serviceability assessment under vertical component of pedestrian load, *ASCE Journal of*
576 *Structural Engineering* 138 (10) (2012) 1193–1202.
- 577 [48] G. Bertos, D. Childress, S. Gard, The vertical mechanical impedance of the locomotor system during human walking with applications in
578 rehabilitation, in: *Proceeding of the 2005 IEEE Ninth International Conference on Rehabilitation Robotics*, 2005.
- 579 [49] J. Dougill, J. Wright, J. Parkhouse, R. Harrison, Human structure-interaction during rhythmic bobbing, *The Structural Engineer* 84 (22)
580 (2006) 32–39.
- 581 [50] M. Toso, H. Gomes, F. Silva, R. Pimentel, Experimentally fitted biodynamic models for pedestrian-structure interaction in walking situations,
582 *Mechanical Systems and Signal Processing* 72-73 (2015) 590–606.
- 583 [51] F. Venuti, L. Bruno, An interpretative model of the pedestrian fundamental relation, *Comptes Rendus Mecanique* 335 (2007) 194–200.
- 584 [52] Y. Matsumoto, T. Nishioka, H. Shiojiri, K. Matsuzaki, Dynamic design of footbridges, *IABSE Proceedings P17/78 (1978)* 1–15.
- 585 [53] A. Johansson, D. Helbing, P. Shukla, Specification of the social force pedestrian model by evolutionary adjustment to video tracking data,
586 *Advances in Complex Systems* 10 (2017) 271.
- 587 [54] M. Boltes, A. Seyfried, Collecting pedestrian trajectories, *Neurocomputing* 100 (2013) 127–133.
- 588 [55] S. Seer, N. Brändle, C. Ratti, Kinects and human kinetics: A new approach for studying pedestrian behavior, *Transportation Research Part B*
589 *48 (2014)* 212–228.
- 590 [56] A. Corbetta, L. Bruno, A. Muntean, F. Toschi, High statistics measurements of pedestrian dynamics, *Transportation Research Procedia* 2
591 (2014) 96–104.
- 592 [57] A. Corbetta, A. Muntean, K. Vafayi, Parameter estimation of social forces in pedestrian dynamics models via a probabilistic method, *Mathe-*
593 *matical Biosciences and Engineering* 12 (2) (2015) 337–356.

- 594 [58] S. Buchmueller, U. Weidmann, Parameters of pedestrians, pedestrian traffic and walking facilities, Tech. Rep. n. 132, ETH, Zürich (October
595 2006).
- 596 [59] A. Gallupa, D. S. J. Haleb, S. Garniera, A. Kacelnik, J. Krebs, I. Couzin, Visual attention and the acquisition of information in human crowds,
597 PNAS 109 (19) (2012) 72457250.
- 598 [60] T. Robin, G. Antonini, M. Bierlaire, J. Cruz, Specification, estimation and validation of a pedestrian walking behavior model, Transportation
599 Research Part B 43 (2009) 36–56.
- 600 [61] W. Daamen, Modelling passenger flows in public transport facilities, Ph.D. thesis, Delft University of Technology, Department of Transport
601 and Planning (2004).
- 602 [62] Sétra/AFGC, Passerelles piétonnes. Évaluation du comportement vibratoire sous l'action des piétons. (Footbridges. Assessment of vibrational
603 behaviour of footbridges under pedestrian loading) (2006).
- 604 [63] International Organization for Standardization, ISO 10137:2007. Bases for design of structures. Serviceability of buildings and walkways
605 against vibration (2007).
- 606 [64] Research Fund for Coal and Steel, HiVoSS: Design of footbridges (2008).
- 607 [65] A. Salyards, Y. Hua, Assessment of dynamic properties of a crowd model for human-structure interaction modeling, Engineering Structures
608 89 (2015) 103–110.
- 609 [66] D. E. Newland, An Introduction to Random Vibrations: Spectral and Wavelet Analysis, Dover Publications, New York, 2005.